

# Current Transport Properties of 200 A-200 m-Class IBAD YBCO Coated Conductor over Wide Range of Magnetic Field and Temperature

著者	渡辺 和雄
journal or publication title	IEEE Transactions on Applied Superconductivity
volume	17
number	2
page range	3207-3210
year	2007
URL	<a href="http://hdl.handle.net/10097/47179">http://hdl.handle.net/10097/47179</a>

doi: 10.1109/TASC.2007.898925

# Current Transport Properties of 200 A-200 m-Class IBAD YBCO Coated Conductor Over Wide Range of Magnetic Field and Temperature

M. Inoue, T. Kiss, D. Mitsui, T. Nakamura, T. Fujiwara, S. Awaji, K. Watanabe, A. Ibi, S. Miyata, Y. Yamada, and Y. Shiohara

**Abstract**—Current transport properties in 200 A-200 m-class IBAD-YBCO coated conductor (CC) have been investigated over a wide range of temperature and magnetic flux density up to 26 T. YBCO CC fabricated by reel-to-reel pulsed laser deposition equipment with a multi-plume and multi-turn deposition system showed high critical current of 245 A in length of 212.6 m. Critical current density,  $J_c$ , in 5 T parallel to  $c$ -axis at 65 K and 4.2 K were 0.44 MA/cm<sup>2</sup> and 5.5 MA/cm<sup>2</sup>, respectively. Moreover, even in very high magnetic flux density, the superior  $J_c$  property remains at lower temperature, e.g.  $J_c$  at 4.2 K in 26 T was 2 MA/cm<sup>2</sup>. We also showed analytical expressions of electric field vs. current density ( $E$ - $J$ ) characteristics based on a framework of percolation model and scaling law of the flux pinning properties. Using the expressions,  $E$ - $J$  characteristics and  $J_c$  value at any conditions of temperature and magnetic flux density can be predicted quantitatively.

**Index Terms**—Critical current density, high-temperature superconductors, superconducting filaments and wires, superconducting materials measurements, YBCO.

## I. INTRODUCTION

NEXT generation superconducting wires based on  $Y_1Ba_2Cu_3O_{7-\delta}$  (YBCO) superconductor have been developed steadily [1]–[3]. Some groups have succeeded in fabricating over hundred meter long YBCO coated conductor (CC) with high critical current,  $I_c$ , over 200 A/cm-width (A/cm-w), e.g. 322 m  $\times$  212 A/cm-w Sm-doped YBCO CC was developed by Super Power Co. [4], 94 m  $\times$  350 A/cm-w hybrid YBCO CC was fabricated by American Superconductor (AMSC) [5], and 212.6 m  $\times$  245 A/cm-w YBCO CC was fabricated by SRL-Nagoya Coated Conductor Center (NCCC), [6], [7]. Moreover, they already demonstrated superconducting

Manuscript received August 29, 2006. This work was supported in part by the “New Energy and Industrial Technology Development Organization (NEDO) as Collaborative Research and Development of Fundamental Technologies for Superconductivity Applications” and by “JSPS: KAKENHI (18360135)”.

M. Inoue, T. Kiss, D. Mitsui, T. Nakamura, and T. Fujiwara are with the Department of Electrical and Electronic Systems Engineering, Kyushu University, Fukuoka 812-8581, Japan (e-mail: inoue@ees.kyushu-u.ac.jp).

S. Awaji and K. Watanabe are with the High Field Laboratory for Superconducting Materials, Tohoku University, Sendai 980-8577, Japan.

A. Ibi, S. Miyata, and Y. Yamada are with the Nagoya Coated Conductor Center, Superconductivity Research Laboratory, Nagoya 456-8587, Japan.

Y. Shiohara is with the Superconductivity Research Laboratory, Tokyo 135-0062, Japan.

Color versions of one or more of the figures in this paper are available online at <http://ieeexplore.ieee.org>.

Digital Object Identifier 10.1109/TASC.2007.898925

coils using the long length high- $I_c$  CC. These results lead us to next stage of R&D for practical applications such as superconducting motor, transformer, magnet system and so on. However, the current transport characteristics of long length high- $I_c$  CC are not sufficiently investigated yet.

In this study, we investigate the current transport properties in 212.6 m  $\times$  245 A/cm-w YBCO CC [6], [7] over a wide range of temperature and magnetic field. Furthermore, analytical expressions for prediction of transport properties in the YBCO CC are also shown and discussed.

## II. EXPERIMENT

### A. Sample Specification

212.6 m-long YBCO CC with high  $I_c$  of 245 A/cm-w was fabricated by SRL-NCCC in 2005 [6], [7]. 2.25  $\mu$ m thick YBCO film was made by using reel-to-reel pulsed laser deposition equipment with a multi-plume and multi-turn deposition system (MPMT-PLD). Substrate is composed of 3 layers: Hastelloy, Gd<sub>2</sub>Zr<sub>2</sub>O<sub>7</sub> by ion-beam assisted deposition (IBAD), and CeO<sub>2</sub> by PLD.

In order to measure the transport properties in detail, we cut out 1 cm long piece from the long CC and made 70  $\mu$ m wide and 1 mm long microbridge by using photolithograph and wet-etching process.

### B. Measurement of Transport Property

Current vs. voltage ( $I$ - $V$ ) characteristics were measured by conventional dc four-probe method at various conditions of temperature and magnetic field. External magnetic field was applied by using two magnets: superconducting magnet for measurements under 17 T and hybrid magnet system for measurements up to 26 T. The magnetic field angle was parallel or perpendicular to the  $c$ -axis. Bias temperature was controlled by adjusting heater power and flow rate of cooled helium gas, except for 4.2 K. The temperature accuracy was about  $\pm 0.1$  K during the measurements. Critical temperature,  $T_c$  and critical current density,  $J_c$  at 77 K in self-field were 87.5 K and 1.0 MA/cm<sup>2</sup>, respectively, and the values were consistent with those of 1 cm-wide CC.

## III. RESULTS AND DISCUSSIONS

### A. Experimental Results

Fig. 1 shows electric field vs. current density ( $E$ - $J$ ) characteristics at (a) 40 K and (b) 65 K in face-on field,  $B_{\parallel c}$ , and at (c)

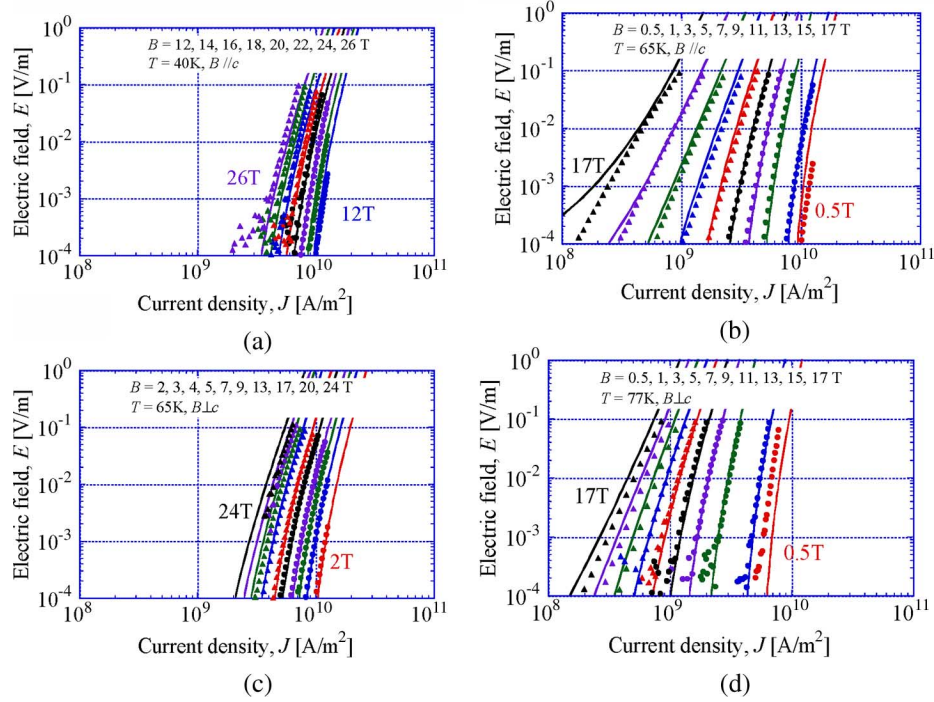


Fig. 1. Magnetic flux density dependences of  $E$ - $J$  characteristics. (a) and (b) are at 40 K and 65 K in  $B_{\parallel c}$ , and (c) and (d) are at 65 K and 77 K in  $B_{\perp c}$ . Symbols and solid lines are experimental results and theoretical solution based on a pinning analysis written in III-B, respectively.

65 K and (d) 77 K in edge-on field,  $B_{\perp c}$ . Experimental data are shown by symbols in Fig. 1. From  $E$ - $J$  characteristics,  $J_c$  -  $B$  property at various temperatures can be obtained as shown in Fig. 2.  $J_c$  was defined by electric field criterion of  $10 \mu\text{V}/\text{cm}$ .  $J_c$  properties in edge-on field are superior to that in face-on field at any temperatures. However, even in face-on magnetic field, high  $J_c$  property is observed at lower temperature, e.g.  $J_c$  at 40 K remains over  $0.5 \text{ MA}/\text{cm}^2$  even in 20 T. Moreover,  $J_c$  at 4.2 K in  $B_{\parallel c}$  is  $2 \text{ MA}/\text{cm}^2$  at 26 T. Since  $1 \text{ MA}/\text{cm}^2$  of  $J_c$  corresponds to  $225 \text{ A}/\text{cm-w}$  of  $I_c$ , high  $I_c$  over  $400 \text{ A}/\text{cm-w}$  can be expected at 4.2 K around 30 T.

### B. Analytical Expression of $E$ - $J$ Characteristics Based on Percolation Model

It has been already shown in our previous works that using statistical distribution parameters of  $J_c$  within a framework of percolation model,  $E$ - $J$  characteristics can be described as follows [8], [9]:

$$E(J) = \frac{\rho_{\text{FF}}}{m+1} J \left( \frac{J}{J_0} \right)^m \left( 1 - \frac{J_{\text{cm}}}{J} \right)^{m+1}, \quad \text{for } J \geq J_{\text{cm}}, \text{ and } B \leq B_{\text{GL}} \quad (1.a)$$

$$= \frac{\rho_{\text{FF}}}{m+1} |J_{\text{cm}}| \left( \frac{|J_{\text{cm}}|}{J_0} \right)^m \left\{ \left( 1 + \frac{J}{|J_{\text{cm}}|} \right)^{m+1} - 1 \right\}, \quad \text{for } J \geq J_{\text{cm}}, \text{ and } B > B_{\text{GL}} \quad (1.b)$$

$$= 0, \quad \text{for } J \leq J_{\text{cm}} \quad (1.c)$$

where,  $J_{\text{cm}}$  is threshold value of percolation transition and  $J_0$  corresponds to half value of  $J_c$  distribution width. The power index  $m$  is a numerical parameter characterizing the shape of  $J_c$  distribution.  $\rho_{\text{FF}}$  is the flux flow resistivity.  $B_{\text{GL}}$  is glass-liquid

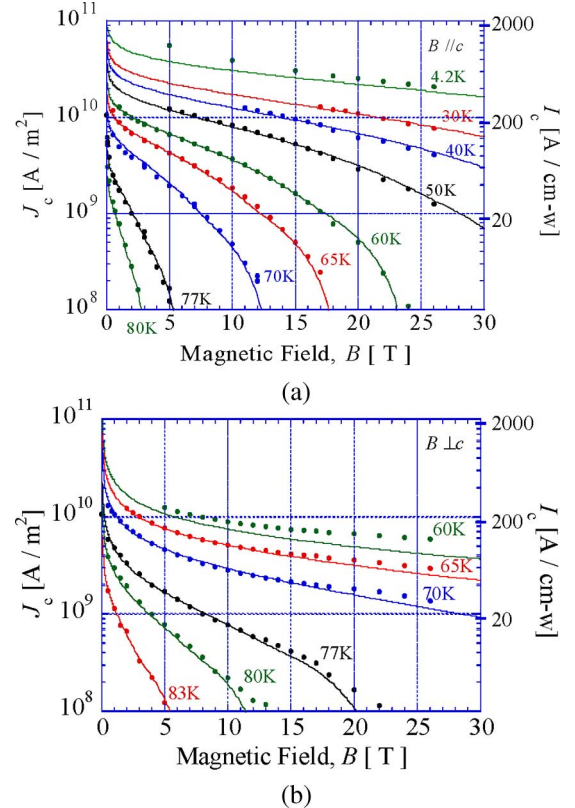


Fig. 2. Magnetic flux density dependences of critical current density,  $J_c$ , at various temperatures. Symbols and solid lines are experimental results and theoretical solutions based on a pinning analysis written in III-B, respectively. (a)  $B_{\parallel c}$ ; (b)  $B_{\perp c}$ .

transition magnetic flux density and defined when  $J_{\text{cm}}$  becomes zero. Using above formulae, we can extrapolate the parameters

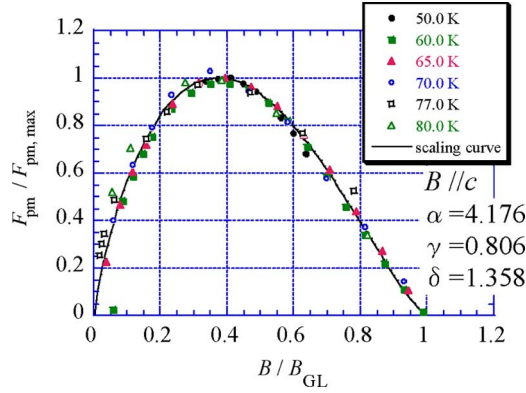


Fig. 3. Scaling property of pinning force density,  $F_{pm}$ , in  $B_{\parallel c}$ . Magnetic flux density dependence of  $F_{pm}$  is scaled on a master curve independently on temperature.

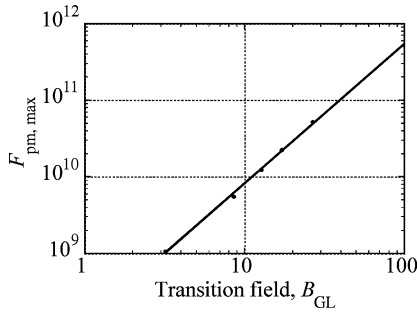


Fig. 4. Transition field,  $B_{GL}$ , dependence of maximum  $F_{pm}$ ,  $F_{pm,max}$  in  $B_{\parallel c}$ . The relationship is expressed by a power function.

from each measured  $E$ - $J$  characteristic. Temperature,  $T$ , and magnetic flux density,  $B$ , dependences of  $J_{cm}$  and  $J_k$  ( $\equiv J_{cm} + J_0$ ) can be obtained by following pinning analysis.

It is known that the minimum strength of pinning force density,  $F_{pm} \equiv J_{cm} \cdot B$ , is scaled on a master curve at wide range of temperature and given as follows [8], [10], [11]:

$$F_{pm} = AB_{GL}^{\zeta} \left( \frac{B}{B_{GL}} \right)^{\gamma} \left( 1 - \frac{B}{B_{GL}} \right)^{\delta} \quad (2)$$

where  $A$ ,  $\zeta$ ,  $\gamma$ , and  $\delta$  are pin parameters. The scaling property of  $F_{pm}$  is shown in Fig. 3. Magnetic flux density dependences of  $F_{pm}$  are well scaled in the temperature range from 50 K to 80 K. Moreover, relationship between peak height value of  $F_{pm}$ , denoted by  $F_{pm,max}$ , and  $B_{GL}$  is expressed as following power function as shown in Fig. 4:

$$F_{pm,max} = \left( \frac{A}{\alpha} \right) B_{GL}^{\zeta}. \quad (3)$$

From the scaling law, the temperature dependence on  $J_{cm}$  can be attributed to the temperature dependence on  $B_{GL}$ .  $B_{GL}$

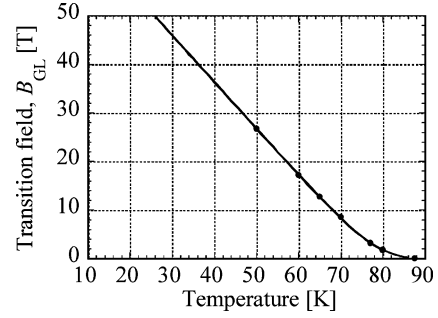


Fig. 5. Temperature dependence on critical magnetic flux density,  $B_{GL}$ , in  $B_{\parallel c}$ .

TABLE I  
NUMERICAL PARAMETERS

Parameter	$J_{cm}$ (B//C)	$J_k$ (B//c)	$J_{cm}$ (B⊥c)	$J_k$ (B⊥c)
$\alpha$	4.18	3.60	2.91	2.22
$\gamma$	0.806	0.793	0.497	0.508
$\delta$	1.36	1.09	1.33	0.659
$A$	$5.14 \times 10^8$	$7.92 \times 10^8$	$3.26 \times 10^8$	$11.4 \times 10^8$
$\zeta$	1.82	2.17	1.39	1.39
$a$	0.139	0.0739	0.0878	0.231
$b$	5.646	10.14	18.83	58.27
$\nu_p$	0.867	0.800	0.860	0.970
$A$ ( $J_{cm} < 0$ )	$1.77 \times 10^8$	-	$9.01 \times 10^7$	-
$\zeta$ ( $J_{cm} < 0$ )	1.67	-	1.81	-
$\delta$ ( $J_{cm} < 0$ )	0.904	-	1.15	-

$$T_c = 87.5 \text{ K}, m = 4.0$$

is described by the following function [10]–[12] as shown in Fig. 5:

$$B_{GL}(T) = \frac{b}{1 - \nu_p} \left( 1 - \frac{T}{T_c} \right) \cdot \left\{ 1 - \frac{a}{1 - T/T_c} + \sqrt{\left( 1 + \frac{a}{1 - T/T_c} \right)^2 - 4\nu_p \cdot \frac{a}{1 - T/T_c}} \right\} \quad (4)$$

where  $a$ ,  $b$  and  $\nu_p$  are numerical parameters.

Scaling property of the typical strength of pinning force density,  $F_{pk} \equiv J_k \cdot B$ , is also obtained using same analysis as  $F_{pm}$ .

Applying all above formulae to measured  $E$ - $J$  characteristics, parameters determining  $J_c$  distribution and pinning scaling can be extrapolated. Parameters extrapolated from experimental results above 50 K in  $B_{\parallel c}$  and above 65 K in  $B_{\perp c}$  under 17 T are shown in Table I. Using those parameters, we can express  $E$ - $J$  characteristics and  $J_c$  property at arbitrary conditions of  $T$  and  $B$  analytically. Calculations are shown by solid lines in Fig. 1 and Fig. 2. We can confirm good agreement with experimental results over a wide range of magnetic flux density up to around 30 T, temperature, and electric field.

#### IV. CONCLUSION

We investigated the transport characteristics in 212.6 m-long and 245 A- $I_c$  YBCO coated conductor in detail including in high magnetic flux density region up to around 30 T. The experimental results confirmed that even in parallel magnetic flux

density to the  $c$ -axis, the YBCO CC maintains high  $J_c$  property at lower temperature e.g.  $J_c$  at 4.2 K in 26 T was higher than  $2 \text{ MA/cm}^2$  and  $J_c$  at 40 K remains over  $0.5 \text{ MA/cm}^2$  even in 20 T. We also showed that transport characteristics at arbitrary conditions of temperature and magnetic flux density can be predicted using analytical expressions based on percolation model together with scaling law of flux pinning property. These results are useful as fundamental data and also for engineering design of practical applications using YBCO CC.

#### REFERENCES

- [1] Y. Shiohara and Y. Aoki, "Activity of R&D for coated conductors in Japan," *Physica C*, vol. 426–431, pp. 1–7, 2005.
- [2] D. F. Lee, H. M. Christen, F. A. List, L. Heatherly, K. J. Leonard, C. M. Rouleau, S. W. Cook, P. M. Martin, M. Paranthaman, and A. Goyal, "R&D of RABiTS-based coated conductors: Conversion of ex situ YBCO superconductor using a novel pulsed electron-beam deposited precursor," *Physica C*, vol. 426–431, pp. 878–886, 2005.
- [3] Y.-Y. Xie, A. Knoll, Y. Chen, Y. Li, X. Xiong, Y. Qiao, P. Hou, J. Reeves, T. Salagaj, K. Kenseth, L. Civale, B. Maiorov, Y. Iwasa, V. Solovyov, M. Suenaga, N. Cheggour, C. Clickner, J. W. Ekin, C. Weber, and V. Selvamanickam, "Progress in scale-up of second-generation high-temperature superconductors at SuperPower Inc," *Physica C*, vol. 426–431, pp. 849–857, 2005.
- [4] V. Selvamanickam, Y.-Y. Xie, and J. Reeves, "Progress in scale-up of 2G conductor at SuperPower," *Supercond. for Electric Systems 2006 Annu. Peer Review*.
- [5] S. Fleshier, A. Malozemoff, and M. Rupich, "Scale-up of 2G HTS wire manufacturing at American superconductor," *Supercond. for Electric Systems 2006 Annu. Peer Review*.
- [6] Y. Yamada, A. Ibi, H. Fukushima, R. Kuriki, S. Miyata, K. Takahashi, H. Kobayashi, S. Ishida, M. Konishi, T. Kato, T. Hirayama, and Y. Shiohara, "Towards the practical PLD-IBAD coated conductor fabrication—Long wire, high production rate and  $J_c$  enhancement in a magnetic field," *Physica C*, in press.
- [7] A. Ibi, Y. Yamada, H. Fukushima, R. Kuriki, S. Miyata, T. Watanabe, and Y. Shiohara, *J. Cryogenic Soc. Jpn.*, pp. 585–592, Dec. 2005.
- [8] K. Yamafuji and T. Kiss, "Current-voltage characteristics near the glass-liquid transition in high-Tc superconductors," *Physica C*, vol. 290, pp. 9–22, Oct. 1997.
- [9] T. Kiss, M. Inoue, S. Egashira, T. Kuga, M. Ishimaru, M. Takeo, T. Matsushita, Y. Iijima, K. Kakimoto, T. Saitoh, S. Awaji, K. Watanabe, and Y. Shiohara, "Percolative transition and scaling of transport  $E - J$  characteristics in YBCO coated IBAD tape," *IEEE Trans. Appl. Supercond.*, vol. 13, no. 2, pp. 2607–2610, Jun. 2003.
- [10] M. Inoue, T. Kiss, T. Kuga, M. Ishimaru, M. Takeo, T. Matsushita, Y. Iijima, K. Kakimoto, T. Saitoh, S. Awaji, K. Watanabe, and Y. Shiohara, "Estimation of  $E - J$  characteristics in a YBCO coated conductor at low temperature and very high magnetic field," *Physica C*, vol. 426–431, pp. 878–886, 2005.
- [11] M. Inoue, T. Kiss, Y. Tsuda, H. Sawa, M. Takeo, S. Awaji, K. Watanabe, Y. Iijima, K. Kakimoto, T. Saitoh, J. Matsuda, Y. Tokunaga, T. Izumi, and Y. Shiohara, "High magnetic field properties of critical current density in  $\text{Y}_1\text{Ba}_2\text{Cu}_3\text{O}_{7-\delta}$  coated conductor fabricated by improved TFA-MOD process," *IEEE Trans. Appl. Supercond.*, vol. 15, no. 2, pp. 2574–2577, Jun. 2005.
- [12] T. Koyama and M. Tachiki, "The effect of internal orbital motion in 2D d-wave superconductors," *Physica C*, vol. 263, pp. 25–29, May 1996.